Available online at www.sciencedirect.com
ScienceDirect
Journal of Organometallic Chemistry 692 (2007) 201–207
Journal of Organometallic Chemistry
www.elsevier.com/locate/jorganchem

Molybdenum complexes bearing a diaminosubstituted-phosphiteboryl ligand: Syntheses, structures, and reactivity involving the Mo–B, B–P, and B–H activation

Hiroshi Nakazawa *, Masumi Itazaki, Masaharu Ohba

Department of Chemistry, Graduate School of Science, Osaka City University, Sumiyoshi-ku, Osaka 558-8585, Japan

Received 24 March 2006; received in revised form 21 April 2006; accepted 24 April 2006
Available online 1 September 2006

Abstract

Photoreaction of diaminosubstituted-phosphiteborane, $BH_3P(NMeCH_2)_2(OMe)$ with a methyl molybdenum complex, $(\eta^5\text{-}C_5R_5)Mo(CO)_3Me$ ($R_5 = Me_5$, Me_4H, H_5) yielded a phosphiteboryl molybdenum complex, $(\eta^5\text{-}C_5R_5)Mo(CO)_3BH_2\{P(NMeCH_2)_2(OMe)\}$ ($R_5 = Me_5$: **2**, Me_4H: **3**, H_5: **4**). In the reaction of **2** with MeI, the Mo–B bond was activated to give $(\eta^5\text{-}C_5Me_5)Mo(CO)_3Me$, in the reaction with PMe_3, the B–P bond was activated to give $(\eta^5\text{-}C_5Me_5)Mo(CO)_3(BH_2PMe_3)$. Complex **2** in solution was gradually converted into $(\eta^5\text{-}C_5Me_5)MoH(CO)_2\{P(NMeCH_2)_2(OMe)\}$ (**8**) via the B–H bond activation of **2**. Structures of **2**, **3**, and **8** were determined by single crystal X-ray diffraction studies.

Keywords: Phosphiteborane; Phosphiteboryl complex; Bond activation; Photoreaction; Molybdenum; X-ray structure

1. Introduction

Phosphineborane ($R_3PBR'_3$) is generally considered to be a Lewis base–acid adduct, that is, the P–B bond consists of donation of lone-pair electrons on the phosphorus to the empty p orbital of the boron. On the other hand, phosphineborane also can be seen as a phosphonium-borate compound with a P–B covalent bond, if positive and negative charge is located on the P and the B, respectively. In the latter description, phosphineborane is isoelectronic to alkane. Phosphineborane may be described as a resonance hybrid somewhere between these two extremes. Phosphideborane complexes ($L_nM\text{-}PR_2BR'_3$) and phosphineboryl complexes ($L_nM\text{-}BR'_2PR_3$) attracted considerable attention. Since phosphideborane complexes are formally produced by the displacement of one substituent on the P of phosphineborane by a transition fragment and phosphineboryl complexes are formally produced by the displacement of one substituent on the B by a transition metal fragment, these complexes are isoelectronic to organo-transition-metal complexes.

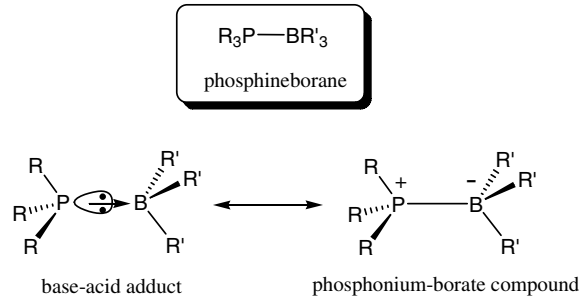

B–H bond activation of BH_3PR_3 with a transition metal complex is a subject of growing interest, because this reaction can be considered as a model reaction of alkane C–H activation [1]. Many examples of B–H bond activation by

* Corresponding author. Tel.: +81 6 6605 2547; fax: +81 6 6605 2522.
E-mail address: nakazawa@sci.osaka-cu.ac.jp (H. Nakazawa).

0022-328X/$ - see front matter © 2006 Elsevier B.V. All rights reserved.
doi:10.1016/j.jorganchem.2006.04.049

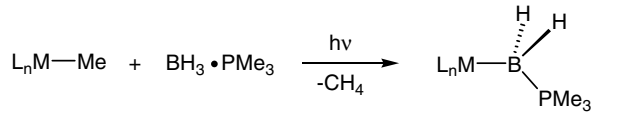

Scheme 1.

transition metal complexes have been reported for tri-coordinate boranes [2,3]. In contrast, little is known of B–H bond activation of tetra-coordinate (sp^3-type) boranes such as $BH_3 \cdot PR_3$ [4,5]. Shimoi et al. reported elegant examples of B–H bond activation of tetra-coordinate borane (Scheme 1). The photolysis of $Cp^*M(CO)_3Me$ ($Cp^* = \eta^5$-C_5Me_5, M = Mo, W) in the presence of $BH_3 \cdot PMe_3$ produced $Cp^*M(CO)_3BH_2(PMe_3)$ [6]. They also synthesized $Cp^*M(CO)_2BH_2(PMe_3)$ (M = Fe, Ru) [7] and $Mn(CO)_3(PR_3)BH_2(PMe_3)$ ($PR_3 = PEt_3$, PMe_2Ph) [8]. Shimoi's method, that is, photoreaction of a methyl complex of transition metal with phosphineborane to produce phosphineboryl complex seems to be useful. But examples shown to date are limited only for trimethylphosphineborane. Herein we demonstrate that photoreaction of $Cp^*Mo(CO)_3Me$ and its derivatives in the presence of several phosphorus compounds, such as diaminosubstituted-phosphiteborane, $BH_3P(NMeCH_2)_2(OMe)$ (**1**), produced phosphiteboryl Mo complexes, such as $Cp^*Mo(CO)_3BH_2\{P(NMeCH_2)_2(OMe)\}$ (**2**). We also present the unprecedented reactivity of **2** involving Mo–B bond activation by MeI, B–P bond activation by PMe_3, and B–H bond activation. A part of this work was reported preliminarily [9].

2. Results and discussion

2.1. Synthesis and characterization of phosphiteboryl molybdenum complexes

Treatment of $P(NMeCH_2)_2(OMe)$ [10] with $BH_3 \cdot THF$ yields a diaminosubstituted-phosphiteborane, $BH_3 \cdot P(NMeCH_2)_2(OMe)$ (**1**) in the analogous method [11], as a white solid in 98% yield, as shown in Eq. (1).

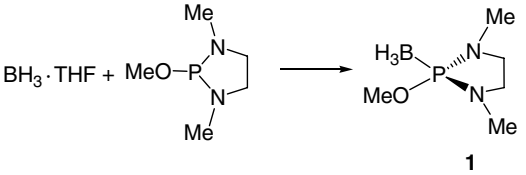

(1)

Photoreaction of **1** with some methyl molybdenum complexes (η^5-C_5R_5)$Mo(CO)_3Me$ ($R_5 = Me_5$, Me_4H, H_5) [12–14] at 0 °C in 1:1 molar ratio afforded corresponding phosphiteboryl complexes (η^5-C_5R_5)$Mo(CO)_3BH_2\{P(NMeCH_2)_2(OMe)\}$ ($R_5 = Me_5$: **2**, Me_4H: **3**, H_5: **4**) (Eq. (2)). The isolation yields were 43% for **2** and 13% for **3**. Complex **4** could not be isolated due to its thermal instability. We sought optimized reaction conditions to get a better isolation yield, and found that the reaction of **1** with a slightly excess amount (1.36 times molar ratio) of $Cp^*Mo(CO)_3Me$ produces **2** in a 70% yield based on the Mo complex and in a 95% yield based on **1**. An analogous methyl complex of another transition metal, $Cp^*W(CO)_3Me$ and $Cp^*M(CO)_2Me$ (M = Fe, Ru), did not react with **1** under the same reaction conditions. This is in contrast to the results of the reaction with $BH_3 \cdot PMe_3$ (see Scheme 1).

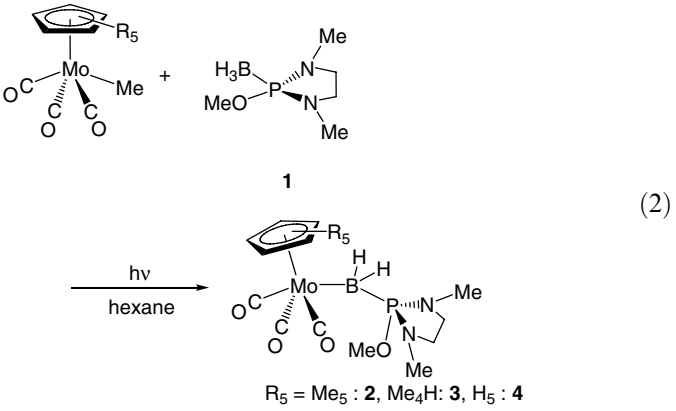

(2)

The X-ray structures of **2** and **3** were determined by X-ray crystallography. The molecular structures of **2** and **3** are shown in Fig. 1(a) and (b), respectively, and selected bond distances and angles are summarized in Table 1. Both complexes have a phosphiteboryl ligand, a C_5R_5 ligand with η^5-fashion ($R_5 = Me_5$: **2**, Me_4H: **3**), and three carbonyl ligands around the Mo forming a four-legged piano-stool structure. The Mo–B bond distance is 2.472(4) Å in **2** and 2.487(3) Å in **3**, and slightly shorter than that of the previously reported phosphineboryl complex, $Cp^*Mo(CO)_3\{BH_2(PMe_3)\}$ (2.497(5) Å) [6]. The B–P bond distance (1.903(4) Å: **2**, 1.908(3) Å: **3**) is obviously shorter than that of the corresponding phosphineboryl complexes, $Cp^*M(CO)_3\{BH_2(PMe_3)\}$ (M = Mo: 1.949(5) Å, W: 1.952(7) Å) [6]. The bond distances of Mo–C(carbonyl) are almost the same for **2**, **3**, and $Cp^*Mo(CO)_3\{BH_2(PMe_3)\}$, irrespective of the geometrical position of CO (cis or trans to the boryl ligand). The bond angles of Mo–B–P (123.4(2)° for **2**, 121.2(1)° for **3**) are similar to that of the phosphineboryl complex (121.4(2)°) [6], showing that these borons have typical tetrahedral geometries.

The $^{31}P\{^1H\}$ NMR signals in **1**-**3** show broad quartet at δ 113.3 (q, $J_{BP} = 102.1$ Hz) for **1**, 103.6 (q, $J_{BP} = 127.6$ Hz) for **2**, and 103.9 (q, $J_{BP} = 127.2$ Hz) for **3**. In the ^{11}B NMR, the chemical shifts for **2** (δ −29.6, $J_{PB} = 130.0$ Hz, $J_{HB} = 120.4$ Hz) and **3** (δ −30.0, $J_{PB} = 130.0$ Hz, $J_{HB} = 110.7$ Hz) are at lower field than that for **1** (δ −42.2, dq, $J_{PB} = 102.1$ Hz, $J_{HB} = 96.3$ Hz). The similar tendency has been observed for $Cp^*Mo(CO)_3\{BH_2(PMe_3)\}$ [6].

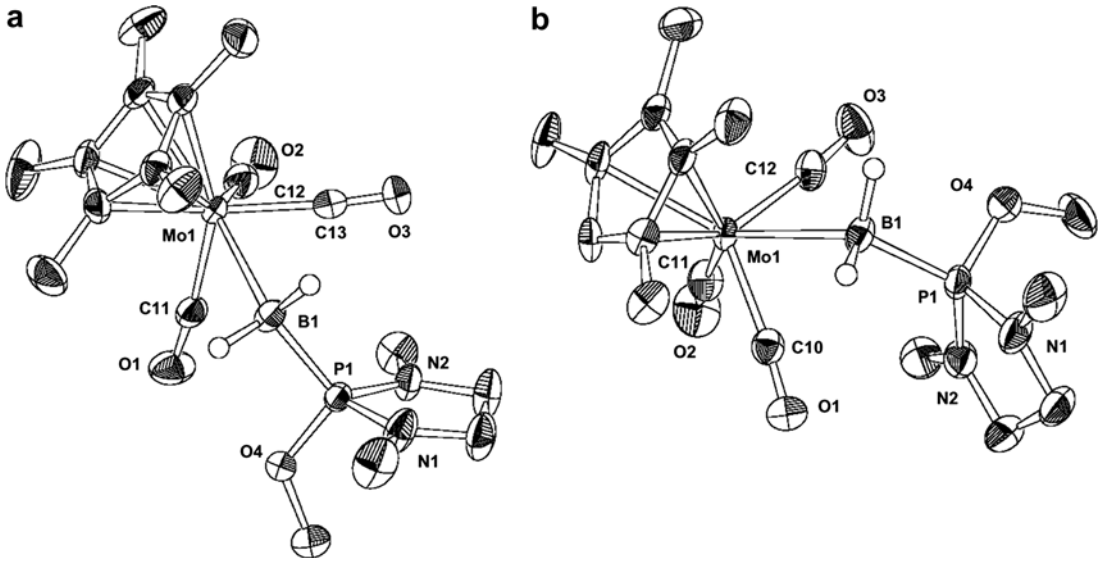

Fig. 1. ORTEP drawing of (a) **2**, and (b) **3** at 30% thermal ellipsoidal plots. The hydrogen atoms are omitted for simplicity.

Table 1
Selected bond lengths (Å) and angles (°) for **2** and **3**

	2	**3**
Bond lengths (Å)		
Mo(1)–B(1)	2.472(4)	2.487(3)
Mo(1)–C(11) (C(10) for **3**)	1.975(4)	1.961(3)
Mo(1)–C(12) (C(11) for **3**)	1.964(4)	1.964(3)
Mo(1)–C(13) (C(12) for **3**)	1.973(4)	1.971(3)
B(1)–P(1)	1.903(4)	1.908(3)
P(1)–O(4)	1.604(3)	1.607(2)
P(1)–N(1)	1.642(3)	1.646(3)
P(1)–N(2)	1.652(3)	1.641(2)
O(1)–C(11) (C(10) for **3**)	1.132(5)	1.145(3)
O(2)–C(12) (C(11) for **3**)	1.153(5)	1.154(4)
O(3)–C(13) (C(12) for **3**)	1.145(5)	1.146(4)
Bond angles (°)		
B(1)–Mo(1)–C(11) (C(10) for **3**)	73.0(1)	67.21(10)
B(1)–Mo(1)–C(12) (C(11) for **3**)	129.3(2)	125.8(1)
B(1)–Mo(1)–C(13) (C(12) for **3**)	66.3(2)	69.00(10)
Mo(1)–B(1)–P(1)	123.4(2)	121.2(1)
B(1)–P(1)–O(4)	105.6(2)	104.3(1)
B(1)–P(1)–N(1)	113.8(2)	113.1(1)
B(1)–P(1)–N(2)	124.0(2)	126.1(1)
N(1)–P(1)–N(2)	93.3(2)	93.1(1)
N(1)–P(1)–O(4)	110.9(2)	113.5(1)
N(2)–P(1)–O(4)	108.8(2)	106.8(1)

In the IR spectra, **2** and **3** exhibit two absorptions due to CO stretching at 1966, 1880 cm^{-1} for **2**, and 1961, 1871 cm^{-1} for **3**. These ν(CO) values are at 47–58 cm^{-1} lower frequency than those for $Cp^*Mo(CO)_3(Me)$ (2008, 1929 cm^{-1}), and at 24–37 cm^{-1} higher frequency than those for the phosphineboryl complex (1942, 1843 cm^{-1}). It has been reported that polarization of the $M^{\delta-}$–$B^{\delta+}$ in a phosphineboryl complex is strong [6]. The above IR data suggest that $M^{\delta-}$–$B^{\delta+}$ polarization is expected for **2** and **3** but the extent is not as great as that of the phosphineboryl complex.

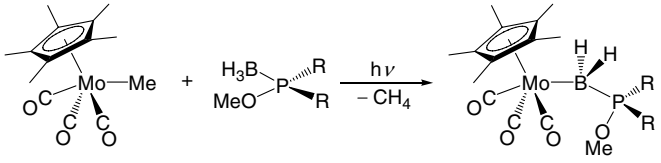

		^{11}B	^{31}P		^{11}B	^{31}P
R = NEt_2	**5**	-40.9	121.2	**5'**	-31.3	112.5
R = Ph	**6**	-40.1	109.8	**6'**	-29.9	106.0
R = OMe	**7**	-45.7	121.1	**7'**	-35.6	108.9

Scheme 2.

Photoreactions of other phosphorus-boron adducts, $BH_3P(OMe)R_2$ (R = NEt_2: **5** [15], Ph: **6** [16], OMe: **7** [15,17]) with $Cp^*Mo(CO)_3Me$ were examined. The formations of the corresponding boryl complexes 5′–7′ were suggested on the basis of the ^{11}B and ^{31}P NMR data (Scheme 2). However, these complexes could not be isolated due to their thermal instability. In the same reaction conditions, $BH_3P(OPh)_3$ did not react with $Cp^*Mo(CO)_3Me$.

2.2. Reaction of 2 with MeI and PMe_3

The reaction of **2** with MeI yielded $Cp^*Mo(CO)_3Me$ and $BH_2I \cdot P(NMeCH_2)_2(OMe)$ (Eq. (3)). This reaction is similar to that shown by $Cp^*Mo(CO)_3\{BH_2(PMe_3)\}$ and is explained by the $M^{\delta-}$–$B^{\delta+}$ polarization. The reaction of $Cp^*Mo(CO)_3\{BH_2(PMe_3)\}$ with HCl, Me_3SiCl, and PMe_3 has been reported to cause the Mo–B bond cleavage. But the B–P bond cleavage has not been

reported. Complex **2** showed such reactivity in the reaction with an equimolar amount of PMe_3. The products were $Cp^*Mo(CO)_3\{BH_2(PMe_3)\}$ and free $P(NMeCH_2)_2(OMe)$ (Eq. (4)). This phosphite/phosphine exchange reaction is quantitative according to the ^{31}P NMR measurements. It should be noted that $Cp^*Mo(CO)_3\{BH_2(PMe_3)\}$ reacts with PMe_3 to give $[Cp^*Mo(CO)_3]^-[H_2B(PMe_3)_2]^+$ where the Mo–B bond is cleaved [6], whereas **2** reacts with PMe_3 to give $Cp^*Mo(CO)_3\{BH_2(PMe_3)\}$ where the B–P bond is cleaved.

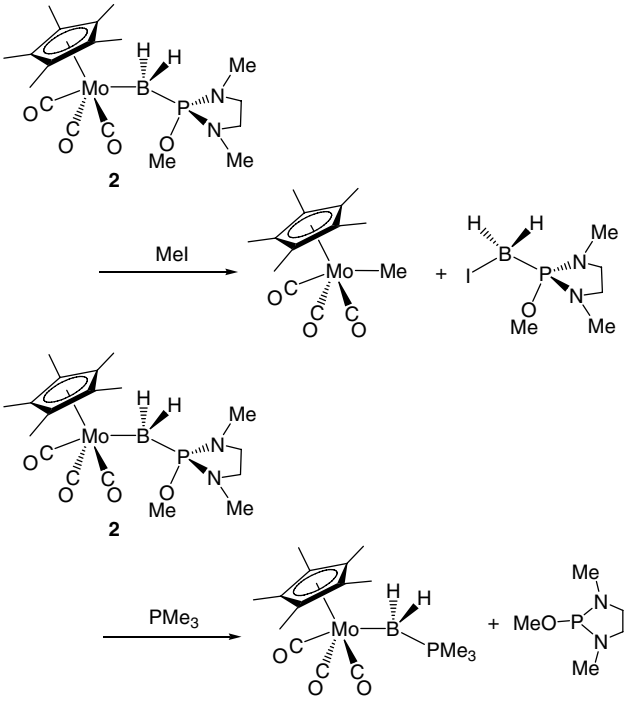

(3)

(4)

2.3. B–H bond activation of 2

Complex **2** is stable in the solid state unless it is exposed to air. However, **2** is gradually converted into a hydride phosphite complex $Cp^*MoH(CO)_3\{P(NMeCH_2)_2(OMe)\}$ (**8**) in solution (Eq. (5)). The C_6D_6 solution of **2** was monitored by the NMR measurements. In the ^{31}P NMR, the quartet at 103.6 ppm due to **2** decreased in intensity and finally disappeared, instead a singlet at 183.6 ppm (a doublet with $J_{PH} = 62.7$ Hz in the proton-coupled measurement) appeared. In the ^1H NMR, a distinctive doublet attributable to a hydride ligand appeared at −5.81 ppm ($J_{PH} = 62.7$ Hz). The conversion was completed within 24 h at room temperature, and was quantitative according to the ^{31}P NMR monitoring. The quantitative conversion of **2** into **8** was reproducible, suggesting that the hydrogen in **8** comes from that on the B in **2** and not from contaminated water. In the ^{11}B NMR, no new signals were observed, so the fate of boron in this reaction was not clear. It was also found that **8** can be prepared from $Cp^*Mo(CO)_3H$ and P $(NMeCH_2)_2(OMe)$ (Eq. (6)) [18,19], and characterized by the X-ray structure analysis.

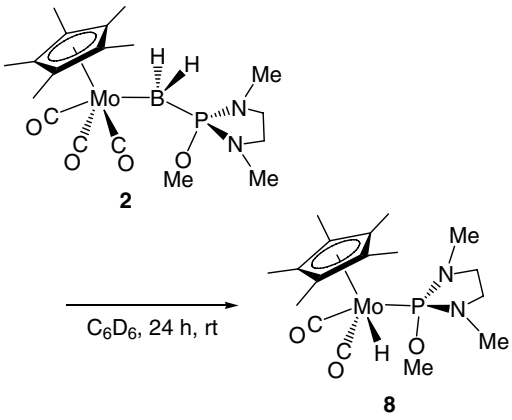

(5)

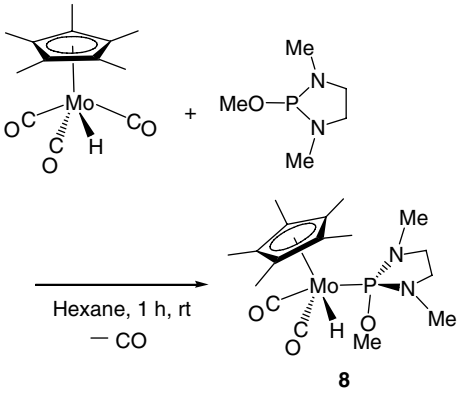

(6)

The molecular structure of **8** was confirmed by the X-ray analysis and was consistent with that estimated from the NMR data. The ORTEP drawing is shown in Fig. 2 and selected bond distances and angles are listed in Table 2. Complex **8** takes a typical four-legged piano-stool geometry. The hydride ligand is situated at the *cis* position to the phosphite ligand. The structural disorder was observed in the OMe group on the P atom. Two Mo–C(carbonyl) bond distances are similar each other (1.952(5), 1.957(5) Å). The Mo–P bond distance (2.3715(14) Å) is shorter than that in a cationic phosphenium molybdenum

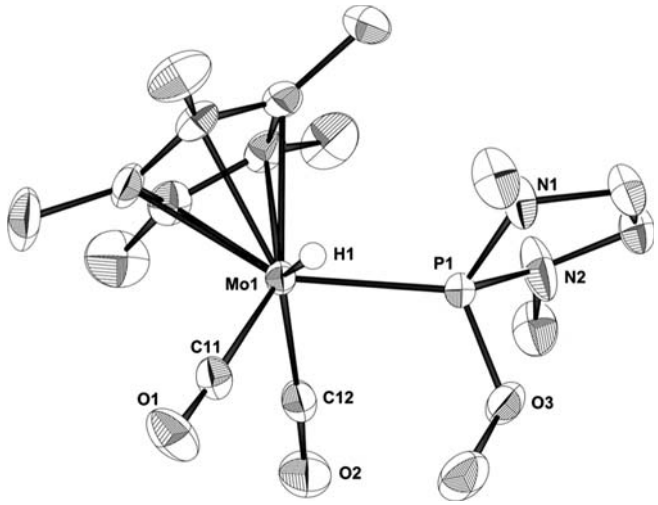

Fig. 2. ORTEP drawing of **8** at 50% thermal ellipsoidal plots. The hydrogen atoms except for the hydride ligand are omitted for simplicity.

Table 2
Selected bond lengths (Å) and angles (°) for **8**

Bond lengths (Å)	
Mo(1)–P(1)	2.3715(14)
Mo(1)–H(1)	1.69(8)
Mo(1)–C(11)	1.952(5)
Mo(1)–C(12)	1.957(5)
P(1)–N(1)	1.672(4)
P(1)–N(2)	1.675(5)
C(11)–O(1)	1.155(6)
C(12)–O(2)	1.157(6)
Bond angles (°)	
C(11)–Mo(1)–P(1)	108.75(14)
C(12)–Mo(1)–P(1)	83.57(14)
C(11)–Mo(1)–C(12)	80.4(2)
C(11)–Mo(1)–H(1)	70(3)
C(12)–Mo(1)–H(1)	130(3)
H(1)–Mo(1)–P(1)	69(3)
Mo(1)–P(1)–N(1)	119.09(16)
Mo(1)–P(1)–N(2)	120.15(19)
N(1)–P(1)–N(2)	91.2(2)

complex having same phosphite ligand (2.495(1) Å) [21]. The ^{1}H NMR signal attributable to the hydride ligand in **8** appears at δ −5.81 (^2J(HP) = 62.7 Hz). The ^2J(HP) value is in the range of the reported values for H–Mo(Cp)–P complexes (56.7–65.7 Hz for *cis* geometry) [22]. Therefore, the hydride and phosphite ligands in **8** are concluded to be mutually *cis* even in solution. The ^{31}P{^{1}H} NMR spectrum of **8** shows a singlet (a doublet with ^2J(PH) = 62.7 Hz in the proton-coupled measurement) at 183.6 ppm.

Two reaction pathways from **2** to **8** are conceivable (Scheme 3). One possibility is shown in Pathway A. Complex **2** may be in equilibrium in solution with [Cp*Mo(CO)$_3$]$^-$[BH$_2$P(NMeCH$_2$)$_2$(OMe)]$^+$. Although the latter cannot be detected spectroscopically, the equilibrium seems to be reasonable from the reaction of **2** with MeI (Eq. (3)). [Cp*Mo(CO)$_3$]$^-$ thus formed nucleophilically attacks one of hydrogens on the B in [BH$_2$P(NMeCH$_2$)$_2$(OMe)]$^+$ to give Cp*Mo(CO)$_3$H and P(NMeCH$_2$)$_2$(OMe). Then, one CO ligand in Cp*Mo(CO)$_3$H is replaced by P(NMeCH$_2$)$_2$(OMe) to give **8** as shown in Eq. (6). The other possibility is shown in Pathway B. Cp*Mo(CO)$_3$ and H fragments on the B in **2** are directly coupled to give Cp*Mo(CO)$_3$H, which then reacts with P(NMeCH$_2$)$_2$(OMe) formed in solution to give **8**. The reaction mechanism is not clear now, but the B–H bond in **2** is cleaved and this type of reaction has not been reported for the corresponding trimethylphosphineboryl complex [20]. Therefore, it is characteristic for a phosphiteboryl complex. The conversion from **1** to **8** through **2** shows double B–H bond activation, which is unprecedented for tetracoordinated (sp^3-type) boranes.

3. Experimental

3.1. General remarks

All reactions were carried out under an atmosphere of dry nitrogen by using standard Schlenk tube techniques. Hexane and pentane were distilled from sodium metal and were stored under nitrogen atmosphere. Other solvents were distilled from appropriate drying agents under dry nitrogen prior to use. P(NMeCH$_2$)$_2$(OMe) [10], Cp*Mo(CO)$_3$Me [12], (η^5-C$_5$Me$_4$H)Mo(CO)$_3$Me [13], (η^5-C$_5$H$_5$)Mo(CO)$_3$Me [14], and Cp*Mo(CO)$_3$H [15] were synthesized according to the reported procedures. NMR spectra (^{1}H, ^{11}B, ^{13}C, ^{31}P) were measured on JEOL LA-300 multinuclear spectrometer and JEOL JNM-AL400 spectrometer at 25 °C. ^{1}H and ^{13}C NMR data were referred to residual peaks of solvent as an internal standard. Peak positions of the ^{11}B and ^{31}P NMR spectra were referenced to an external BF$_3$ · OEt$_2$ and 85% H$_3$PO$_4$, respectively. IR spectra were recorded on a Perkin Elmer FTIR-Spectrum one. Photoirradiation was performed at 0 °C with a 400 W medium-pressure mercury arc lamp of Riko UVL-400HA.

3.2. Synthesis of BH$_3$P(NMeCH$_2$)$_2$(OMe) (1)

A THF solution of BH$_3$ · THF (1.15 M, 30 mL, 36 mmol) was slowly added to a solution of P(NMeCH$_2$)$_2$(OMe) (3.56 g, 24 mmol) in pentane (30 mL) at −78 °C, and the mixture was stirred for 5 h at ambient temperature. Volatile materials were removed under reduced pressure, and the resulting residue was washed with a small amount of hexane, collected by filtration, and dried in vacuo to give a white solid of **1** (4.00 g, 23.5 mmol, 98%).

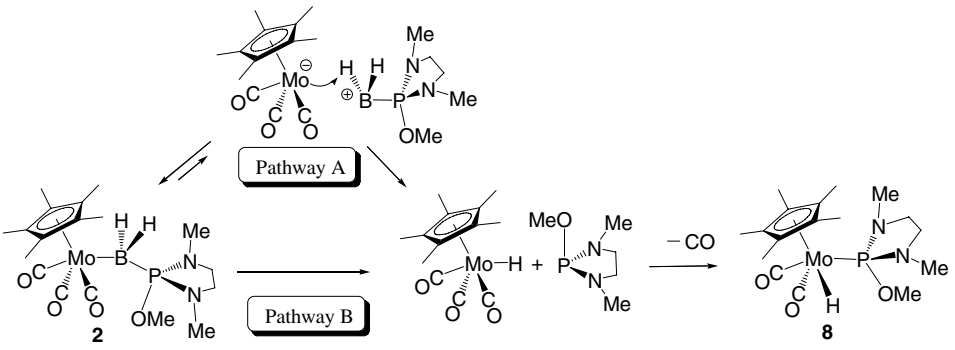

Scheme 3.

^{1}H NMR (400 MHz, $CDCl_3$, δ, ppm): 0.41 (dq, $J_{PH} = 17.3$ Hz, $J_{BH} = 96.3$ Hz, 3H, BH_3), 2.70 (d, $J_{PH} = 10.5$ Hz, 6H, NCH_3), 3.08–3.16 (m, 2H, CH_2), 3.24–3.34 (m, 2H, OCH_3), 3.42 (d, $J_{PH} = 11.0$ Hz, 3H, OCH_3). ^{11}B NMR (128.4 MHz, $CDCl_3$, δ, ppm): −42.2 (dq, $J_{PB} = 102.1$ Hz, $J_{HB} = 96.3$ Hz). ^{13}C{^{1}H} NMR (100.4 MHz, $CDCl_3$, δ, ppm): 32.3 (d, $J_{PC} = 9.3$ Hz, NCH_3), 50.2 (s, OCH_3), 51.4 (d, $J_{PC} = 10.0$ Hz, CH_2). ^{31}P{^{1}H} NMR (161.9 MHz, $CDCl_3$, δ, ppm): 113.3 (q, $J_{BP} = 102.1$ Hz). Anal. Calc. for $C_5H_{16}BN_2OP$: C, 37.08; H, 9.96; N, 17.29. Found: C, 36.88; H, 10.08; N, 16.81%.

3.3. Synthesis of $Cp^*Mo(CO)_3BH_2\{P(NMeCH_2)_2(OMe)\}$ (2)

A hexane solution (15 mL) containing $Cp^*Mo(CO)_3Me$ (495 mg, 1.50 mmol) and $BH_3P(NMeCH_2)_2(OMe)$ (**1**) (178 mg, 1.10 mmol) was subjected to a photoirradiation for 3 h at 0 °C. Removing volatile materials under reduced pressure led to the formation of an orange solid, which was washed with hexane, collected by filtration, and dried in vacuo to give an orange powder of **2** (500 mg, 1.05 mmol, 70%/Mo, 95%/**1**). Orange crystals of complex **2** suitable for an X-ray diffraction study were obtained by cooling the hexane solution at −20 °C for a few days.

^{1}H NMR (300 MHz, C_6D_6, δ, ppm): 1.93 (s, 15H, CCH_3), 2.41–2.69 (m, 4H, CH_2), 2.56 (d, $J_{PH} = 9.3$ Hz, 6H, NCH_3), 2.93 (d, $J_{PH} = 11.2$ Hz, 3 H, OCH_3). ^{11}B NMR (96.3 MHz, C_6D_6, δ, ppm): − 29.6 (dt, $J_{PB} = 130.0$ Hz, $J_{HB} = 120.4$ Hz). ^{13}C{^{1}H} NMR (75.3 MHz, C_6D_6, δ, ppm): 10.7 (s, CCH_3), 32.6 (d, $J_{PC} = 7.5$ Hz, NCH_3), 49.7 (s, OCH_3), 50.2 (d, $J_{PC} = 15.1$ Hz, CH_2), 102.6 (s, CCH_3), 235.1 (br, CO), 236.0 (s, CO). ^{31}P{^{1}H} NMR (121.5 MHz, C_6D_6, δ, ppm): 103.6 (q, $J_{BP} = 127.6$ Hz). IR (cm^{-1}, hexane): ν(CO) 1966 (s), 1880 (s). Anal. Calc. for $C_{18}H_{30}BN_2O_4PMo$: C, 45.40; H, 6.35; N, 5.88. Found: C, 45.17; H, 6.19; N, 5.56%.

3.4. Synthesis of $(\eta^5\text{-}C_5Me_4H)Mo(CO)_3BH_2\{P(NMeCH_2)_2(OMe)\}$ (3)

A hexane solution (25 mL) containing (η^5-C_5Me_4H)-$Mo(CO)_3(Me)$ (810 mg, 2.56 mmol) and $BH_3P(NMeCH_2)_2(OMe)$ (**1**) (332 mg, 2.56 mmol) was subjected to a photoirradiation for 3 h at 0 °C. Removing volatile materials under reduced pressure led to the formation of an orange solid, which was washed with pentane, collected by filtration, and dried in vacuo to give an orange powder of **3** (159 mg, 0.33 mmol, 13%). Orange crystals of complex **3** suitable for an X-ray diffraction study were obtained by cooling hexane solution at −20 °C for a few days.

^{1}H NMR (400 MHz, C_6D_6, δ, ppm): 1.92 (s, 6H, 1,4- or 2,3-CCH_3), 2.00 (s, 6H, 1,4- or 2,3-CCH_3), 2.58–2.74 (m, 4H, CH_2), 2.62 (d, $J_{PH} = 9.3$ Hz, 6H, NCH_3), 3.00 (d, $J_{PH} = 11.2$ Hz, 3H, OCH_3), 4.90 (s, 1H, C_5Me_4H). ^{11}B NMR (128.4 MHz, C_6D_6, δ, ppm): −30.0 (dt, $J_{PB} = 130.0$ Hz, $J_{HB} = 110.7$ Hz). ^{13}C{^{1}H} NMR (100.4 MHz, C_6D_6, δ, ppm): 10.4 (s, 1,4- or 2,3-CCH_3), 12.5 (s, 1,4- or 2,3-CCH_3), 32.5 (d, $J_{PC} = 8.7$ Hz, NCH_3), 49.7 (s, OCH_3), 50.3 (d, $J_{,PC} = 12.1$ Hz, CH_2), 89.3 (s, 5-C_5Me_4H), 103.0 (s, 1,4- or 2,3-CCH_3), 105.3 (s, 1,4- or 2,3-CCH_3), 234.6 (br, CO), 234.9 (s, CO). ^{31}P{^{1}H} NMR (161.9 MHz, C_6D_6, δ, ppm): 103.9 (q, $J_{BP} = 127.2$ Hz). IR (cm^{-1}, hexane): ν(CO) 1961 (s), 1871 (s). Anal. Calc. for $C_{17}H_{28}N_2BO_4PMo$: C, 44.18; H, 6.11; N, 6.06. Found: C, 43.82; H, 6.06; N, 5.73%.

3.5. Reaction of phosphorus · boron adduct (5-7) with $Cp^*Mo(CO)_3Me$

To a heptane solution (10 mL) of $Cp^*Mo(CO)_3Me$ in a Schlenk tube was added an equimolar amount of **5**, $P(NEt_3)_2(OMe)$, and the photoirradiation was performed for several hours. The formation of the corresponding boryl complex **5′** was confirmed by the ^{31}P and ^{11}B NMR spectra. Complex **5′** could not be isolated due to its instability. The adducts **6** and **7** showed the same reactivity.

^{11}B NMR (96.3 MHz, hexane, δ, ppm): **5**: −40.9 (d, $J_{PB} = 95.3$ Hz); **5′**: −31.3 (d, $J_{PB} = 116.5$ Hz); **6**: −40.1 (d, $J_{PB} = 59.7$ Hz); **6′**: −29.9 (d, $J_{PB} = 73.2$ Hz); **7**: –45.7 (d, $J_{PB} = 94.2$ Hz); **7′**: −35.6 (d, $J_{PB} = 128.5$ Hz). ^{31}P NMR (121.5 MHz, hexane, δ, ppm): **5**: 121.2 (q, $J_{BP} = 93.6$ Hz); **5′**: 112.5 (q, $J_{BP} = 113.0$ Hz); **6**: 109.8 (q, $J_{BP} = 59.5$ Hz); **6′**: 106.0 (q, $J_{BP} = 74.1$ Hz); **7**: 121.1 (q, $J_{BP} = 95.6$ Hz); **7′**: 108.9 (q, $J_{BP} = 125.0$ Hz).

3.6. Synthesis of $Cp^*Mo(CO)_3H\{P(NMeCH_2)_2(OMe)\}$ (8)

To a solution of $Cp^*Mo(CO)_3H$ (3.09 g, 9.77 mmol) in hexane (30 mL) was added $P(NMeCH_2)_2(OMe)$ (1.6 mL, 10.0 mmol) at room temperature (Caution! The considerable amount of CO gas was generated by this reaction). After 1 h, volatile materials were removed under reduced pressure. The resulting orange brown materials were dissolved in 2 mL of hexane. After cooling at −78 °C, the reaction mixture led to the formation of an orange solid, which was washed with 2 mL of hexane at −78 °C, collected by filtration, and dried in vacuo to give an orange powder of **8** (3.62 g, 8.30 mmol, 85%). Yellow crystals of complex **8** suitable for an X-ray diffraction study were obtained by cooling the pentane solution at −20 °C for a few days.

^{1}H NMR (400 MHz, C_6D_6, δ, ppm): −5.81 (d, $J_{HP} = 62.7$ Hz, 1H, MoH), 1.89 (s, 15H, CCH_3), 2.62 (d, $J_{HP} = 11.6$ Hz, 6H, NCH_3)s, 2.71 (m, 2H, CH_2), 2.90 (m, 2H, CH_2), 3.04 (d, $J_{HP} = 11.6$ Hz, 3H, OCH_3). ^{13}C{^{1}H} NMR (100.4 MHz, C_6D_6, δ, ppm): 11.3 (s, CCH_3), 33.5 (d, $J_{CP} = 10.6$ Hz, NCH_3), 51.2 (d, $J_{CP} = 5.3$ Hz, OCH_3), 52.2 (d, $J_{CP} = 6.8$ Hz, CH_2), 103.0 (s, CCH_3), 241.5 (br, CO). ^{31}P{^{1}H} NMR (161.9 MHz, C_6D_6, δ, ppm): 183.6 (s). IR (cm^{-1}, C_6D_6): ν(CO) 1930 (s), 1851 (s). Anal. Calc.

Table 3
Crystal data and details of structure refinement of complexes of **2**, **3**, and **8**

	2	**3**	**8**
Empirical formula	$C_{18}H_{30}N_2BO_4PMo$	$C_{17}H_{28}N_2BO_4PMo$	$C_{17}H_{29}N_2O_3PMo$
Formula weight	476.17	462.14	436.34
Crystal system	Monoclinic	Monoclinic	Triclinic
Crystal size (mm^3)	$0.50 \times 0.35 \times 0.05$	$0.45 \times 0.30 \times 0.25$	$0.30 \times 0.08 \times 0.17$
Temperature (K)	200(1)	200(1)	203(2)
Space group	$P2_1/n$ (No. 14)	$P2_1/n$ (No. 14)	$P\bar{1}$ (No. 2)
a (Å)	9.2680(2)	9.1560(1)	8.829(4)
b (Å)	14.5460(4)	21.9100(3)	8.886(4)
c (Å)	17.1080(5)	10.5680(1)	13.847(5)
α (°)			90.660(4)
β (°)	105.371(1)	95.568(1)	101.191(7)
γ (°)			111.629(9)
V (Å^3)	2223.9(1)	2110.2(4)	986.6(6)
Z	4	4	2
μ (mm^{-1})	68.4	71.9	76.2
D_{calcd} (g cm^{-1})	1.422	1.455	1.469
Number of unique reflections	5318	5011	4349
Number of used reflections	4600	4804	4211
Number of variables	245	236	238
R	0.042	0.036	0.048
R_W	0.085	0.095	0.121
Goodness-of-fit	1.48	1.80	1.17

for $C_{17}H_{29}N_2O_3PMo$: C, 46.79; H, 6.70; N, 6.42. Found: C, 46.62; H, 6.71; N, 6.21%.

3.7. X-ray diffraction structure analyses

Crystals of **2**, **3**, and **8** suitable for X-ray diffraction study were mounted in glass capillaries. Data for **2** and **3** were collected at −73 °C on Rigaku RAXIS-IV imaging plate diffractometer equipped with monochromated Mo Kα radiation. Calculations for **2** and **3** were performed with the teXsan crystallographic software package of Molecular Structure Corporation. Data for **8** were collected at −70 °C on Rigaku AFC-7/Mercury CCD area-detector diffractometer equipped with monochromated Mo Kα radiation. Calculations for **8** were performed with the CrystalClear software package of Molecular Structure Corporation. A full-matrix least-squares refinement was used for the non-hydrogen atoms with anisotropic thermal parameters. Hydrogen atoms except for the MoH hydrogen of **8** were located by assuming the ideal geometry and were included in the structure calculation without further refinement of the parameters. Crystal data, details of data collections and refinement are given in Table 3.

Acknowledgements

This work was supported by a Grant-in-Aid (No.15205010), by a Grant-in-Aid for Science Research on Priority Areas (No. 16033250, Reaction Control of Dynamic Complexes) from the Ministry of Education, Culture, Sports, Science and Technology, Japan, and by the Yamada Science Foundation.

Appendix A. Supplementary data

Crystallographic data for the structural analyses have been deposited with the Cambridge Crystallographic Data Centre, CCDC Nos. 299004, 299005, and 268038 for **2**, **3**, and **8**, respectively. Copies of this information may be obtained free of charge from the Director, CCDC, 12 Union Road, Cambridge CB2 1EZ, UK (fax: +44 1223 336 033; e-mail: deposit@ccdc.cam.ac.uk or http://www.ccdc.cam.ac.uk). Supplementary data associated with this article can be found, in the online version, at doi:10.1016/j.jorganchem.2006.04.049.

References

[1] A.E. Shilov, G.B. Shul'pin, Chem. Rev. 97 (1997) 2879.
[2] K. Burgess, M.J. Ohlmeyer, Chem. Rev. 91 (1991) 1179.
[3] H. Braunschweig, M. Colling, Coord. Chem. Rev. 223 (2001) 1.
[4] J.D. Basil, A.A. Aradi, N.K. Bhattacharyya, N.P. Rath, C. Eigenbrot, T.P. Fehlner, Inorg. Chem. 29 (1990) 1260.
[5] D.J. Elliot, C.J. Levy, R.J. Puddephatt, D.G. Holah, A.N. Hughes, V.R. Magnuson, I.M. Moser, Inorg. Chem. 29 (1990) 5014.
[6] Y. Kawano, T. Yasue, M. Shimoi, J. Am. Chem. Soc. 121 (1999) 11744.
[7] T. Yasue, Y. Kawano, M. Shimoi, Chem. Lett. (2000) 58.
[8] T. Yasue, Y. Kawano, M. Shimoi, Angew. Chem. Int. Ed. 42 (2003) 1727.
[9] H. Nakazawa, M. Ohba, M. Itazaki, Organometallics 25 (2006) 2903.
[10] F. Ramirez, A.V. Patwardhan, H.J. Kugler, C.P. Smith, J. Am. Chem. Soc. 89 (1967) 6276.
[11] F. Hewitt, K. Holliday, J. Chem. Soc. (1953) 530.
[12] C. Roger, M.J. Tudoret, V. Guerchais, C. Lapinte, J. Organomet. Chem. 365 (1989) 347.
[13] J. Zhao, A.M. Santos, E. Herdtweck, F.E. Kuehn, J. Mol. Catal. A: Chem. 222 (2004) 265.
[14] (a) T.S. Piper, G. Wilkinson, J. Inorg. Nucl. Chem. 3 (1956) 104; (b) A. Asdar, M.J. Tudoret, C. Lapinte, J. Organomet. Chem. 349 (1988) 353.
[15] H. Nakazawa, Y. Kadoi, K. Miyoshi, Organometallics 8 (1989) 2851.
[16] B.A. Arbuzov, N.P. Grechkin, Zh. Obshch. Khim. 20 (1950) 107; B.A. Arbuzov, N.P. Grechkin, Chem. Abstr. 44 (1950) 5832.
[17] G. Rana, K. Vyakaranam, B.F. Spielvogel, J.A. Maguire, N.S. Hosmane, Inorg. Chim. Acta 344 (2003) 249.
[18] (a) A. Asdar, C. Lapinte, L. Toupet, Organometallics 8 (1989) 2708; (b) M.-J. Tudoret, M.-L. Robo, C. Lapinte, Organometallics 11 (1992) 1419.
[19] H. Nakazawa, K. Kubo, C. Kai, K. Miyoshi, J. Organomet. Chem. 439 (1992) C42.
[20] The reaction of bis(trimethylphosphine)diborane ($B_2H_4(PMe_3)_2$) with $Co_2(CO)_8$ to give $(CO)_3Co(\mu\text{-}BHPMe_3)(\mu\text{-}CO)Co(CO)_3$ has been reported. M. Shimoi, S. Ikubo, Y. Kawano, K. Katoh, H. Ogino, J. Am. Chem. Soc. 120 (1998) 4222.
[21] H. Nakazawa, Y. Yamaguchi, T. Mizuta, K. Miyoshi, Organometallics 14 (1995) 4173.
[22] T.-Y. Cheng, B.S. Brunschwig, R.M. Bullock, J. Am. Chem. Soc. 120 (1998) 13121.